The Journal of Experimental Biology 206, 2567-2580

doi:10.1242/jeb.00452

Probing the limits to muscle-powered accelerations: lessons from jumping bullfrogs

Thomas J. Roberts* and Richard L. Marsh

Biology Department, Northeastern University, 414 Mugar, 360 Huntington Ave, Boston, MA 02115, USA

*Author for correspondence at present address: Oregon State University, Zoology Department, 3029 Cordley Hall, Corvallis, OR 97331, USA (e-mail: robertst@bcc.orst.edu)

Accepted 10 April 2003

Summary

The function of many muscles during natural movements is to accelerate a mass. We used a simple model containing the essential elements of this functional system to investigate which musculoskeletal features are important for increasing the mechanical work done in a muscle-powered acceleration. The muscle model consisted of a muscle-like actuator with frog hindlimb muscle properties, operating across a lever to accelerate a load. We tested this model in configurations with and without a series elastic element and with and without a variable mechanical advantage. When total muscle shortening was held constant at 30%, the model produced the most work when the muscle operated with a series elastic element and an effective mechanical advantage that increased throughout the contraction (31 J kg^{-1} muscle *vs* 26.6 J kg^{-1} muscle for the non-compliant, constant mechanical advantage configuration). We also compared the model output with the dynamics of jumping bullfrogs, measured by high-speed video analysis, and the length changes of the plantaris muscle, measured by sonomicrometry. This comparison revealed that the length, force and power trajectory of the body of jumping frogs could be accurately replicated by a model of a fully active muscle operating against an inertial load, but only if the model muscle included a series elastic element. Sonomicrometer measurements of the plantaris muscle revealed an unusual, biphasic pattern of shortening, with high muscle velocities early and late in the contraction, separated by a period of slow contraction. The model muscle produced this pattern of shortening only when an elastic element was included.

These results demonstrate that an elastic element can increase the work output in a muscle-powered acceleration. Elastic elements uncouple muscle fiber shortening velocity from body movement to allow the muscle fibers to operate at slower shortening velocities and higher force outputs. A variable muscle mechanical advantage improves the effectiveness of elastic energy storage and recovery by providing an inertial catch mechanism. These results can explain the high power outputs observed in jumping frogs. More generally, our model suggests how the function of non-muscular elements of the musculoskeletal system enhances performance in muscle-powered accelerations.

Supplementary material available on line.

Key words: locomotion, muscle work, muscle power, jumping, frog, *Rana catesbeiana*, elastic, tendon, acceleration.

Introduction

Frog jumping provides an excellent system for investigating the limits to muscle-powered accelerations. Frogs jump farther than they should, if we consider only the power their muscles are capable of producing. The mechanical power required to accelerate the body can be calculated from jump distance, or from high-speed video analysis, and the muscular power available can be determined from the well-known contractile properties of isolated frog muscle. Results from several studies indicate that these two quantities do not agree; the power transferred to the body during a maximal jump actually exceeds the power available from hindlimb muscles (Marsh and John-Alder, 1994; Peplowski and Marsh, 1997; Navas et al., 1999; Wilson et al., 2000). The discrepancy between muscle power-producing capacity and power output is dramatically illustrated if instantaneous power during the jump is calculated. In Cuban tree frogs (*Osteopilus septentrionalis*), peak instantaneous muscle powers are as much as seven times the power available from hindlimb muscles (Peplowski and Marsh, 1997).

The supramaximal powers observed during jumping probably result from the rapid release of strain energy from elastic elements (Marsh, 1994, 1999). Elastic structures can operate as muscle power amplifiers because they are not bound by the constraints on shortening velocity that limit power output of muscle contractile elements (Hill, 1950a; Alexander, 1988). Yet, how and when these elastic elements are stretched

to store the energy of muscular contraction in frog jumping is unclear. Furthermore, although the hypothesis that elastic elements provide the high power outputs of a jump is reasonable, this hypothesis has not been supported by direct measurements of muscle function.

Nature's Olympian jumpers are insects that utilize a catapult-like mechanism to amplify muscle power for jumping. Fleas, click beetles and locusts contract their muscles to load elastic elements in their limbs prior to initiating a jump (Bennet-Clark and Lucey, 1967; Evans, 1972; Bennet-Clark, 1975). A physical or muscular catch mechanism provides the resistance necessary to allow the preloading of elastic elements by muscular contraction. The release of the catch mechanism triggers the explosive release of elastic strain energy and spectacularly high jump power production. These catapult mechanisms produce extraordinary jumping performance because they solve the problem of the mismatch between muscle contractile behavior and the behavior of an accelerating body. Muscles do the most work when they contract slowly, due to the force–velocity relationship, yet jumping involves a very rapid movement. By separating in time the performance of muscular work from the application of mechanical work to the body, the catapult mechanism overcomes intrinsic constraints of skeletal muscle function (Bennet-Clark and Lucey, 1967; Bennet-Clark, 1977). Without a catch mechanism, it is unclear how and when muscular energy might be loaded into elastic elements and whether the temporal redistribution of muscle work can lead to a performance advantage for jumping.

We undertook the present study to determine whether frogs could produce the high power outputs observed during jumping in the absence of a physical catch mechanism for elastic energy storage. Models of jumping have suggested a small benefit of elastic storage and recovery in jumps without a catch mechanism (Alexander, 1995; Bobbert, 2001), although the power amplification is expected to be smaller. We hypothesized that the action of elastic elements in jumping frogs allows muscles to operate, on average, at slower shortening velocities and higher work outputs. To test this hypothesis, we used a combined empirical and modeling approach. Our model of a muscle-powered acceleration consisted of a muscle actuator with typical contractile properties, operating to accelerate an inertial load. We modeled single contractions with and without an in-series tendon and under conditions of variable effective mechanical advantage (EMA) between the muscle and the load. This simple model reproduced the complex mechanical behavior that results from the interaction of muscle–tendon contractile properties and the inertial behavior of an accelerated load. We predicted that the highest accelerations would occur when the muscle operated in series with a compliant tendon. Our empirical measurements consisted of synchronous high-speed video and sonomicrometry measurements in jumping frogs. The pattern of force, velocity and power applied to the body was calculated from the high-speed video recordings and compared with the same parameters measured for the body in the simulated acceleration. Sonomicrometry measurements in the plantaris muscle, an ankle extensor with a large tendon, allowed us to compare the shortening pattern of the frog muscle with the shortening pattern of the muscle in the simulated acceleration. We predicted that the observed pattern of movement of the body and muscle in the jumping frog would be most closely matched by the configuration of the simulated acceleration that produced the most mechanical work.

Our results bear directly on the more general problem of how muscles might function optimally to accelerate loads. Although acceleration is one of the most common functions of skeletal muscle, the pattern of muscle contraction that might be expected to provide maximal mechanical work output during acceleration is relatively unexplored. During acceleration, the load on the contracting muscle continuously changes because, as the mass accelerates, the force produced by the muscles changes due to force–velocity and length–tension effects. The changing muscle force in turn affects the acceleration of the load. Understanding the mechanisms for optimizing performance during accelerations requires an increased knowledge of the nature of the reciprocal interactions between the changing load, the properties of the muscle and the musculoskeletal structures that link the contracting muscle fibers to the load.

Materials and methods

Animals

Bullfrogs (*Rana catesbeiana* L.) were obtained from a commercial supplier (Charles Sullivan Company, Nashville, TN, USA). Animals were maintained in water-filled plastic containers with dry platforms located in the middle of the tank. Animals were housed in a room maintained at approximately 20°C with a 12 h:12 h L:D cycle. The frogs were fed crickets supplemented with calcium and vitamins three times weekly. Measurements were taken within the first two months of captivity from six animals with body masses between 150 g and 380 g. All animal care procedures were in accordance with institutional guidelines and approved by the Institutional Animal Care and Use Committee at Northeastern University.

Sonomicrometry and electromyography

Sonomicrometer crystals and electromyographic (EMG) electrodes were surgically implanted to measure length change and activity, respectively, in the plantaris muscle of six animals. Details of transducer implantation and surgical procedures are similar to those presented previously by Olson and Marsh (1998). Animals were anesthetized by immersion in a bath of MS-222. When the animals had reached a surgical plane of anesthesia, a small incision was made in the skin caudal to the iliosacral joints at approximately the midpoint of the urostyle. Electrodes were routed subcutaneously from this position to the point of implantation.

Small (1 mm) sonomicrometer crystals (Triton Technology, San Diego, CA, USA) were used to measure fascicle segment lengths in the plantaris longus muscle. The plantaris is a

pinnate muscle that acts primarily as an ankle extensor. The tendinous origin of the plantaris muscle is complex, with one portion attaching to the tibiofibula near the knee and two other portions crossing the knee. Thus, some of the muscle may act with a knee flexor moment. Sonomicrometer crystals were aligned along fascicles that were visible and could be traced from the more superficial aponeurosis to the deep aponeurosis near the point of origin of the muscle. A small incision was made in the muscle fascia between visible muscle fascicles. Sonomicrometer crystals were inserted into this space, and fine 6-0 silk suture was used to secure small stainless steel crystal holders to the surface of the muscle. Care was taken to minimize the depth of these sutures and to minimize damage to muscle fibers. Crystals were implanted 10–15 mm apart. A sonomicrometer (Model 120; Triton Technology) was used to measure length changes from the sonomicrometer crystals. The individual pairs of sonomicrometer crystals were calibrated before implantation and corrections entered for the offset error due to the holders and the epoxy lens (Olson and Marsh, 1998).

Bipolar electromyographic electrodes were constructed from 0.076 mm-diameter Teflon-coated stainless steel wire. Wire ends were bared over approximately 1 mm, and the wires were twisted into the 'simple double hook' configuration (Loeb and Gans, 1986). The electrodes were inserted in the region of length measurement using a 25-gauge hypodermic needle. The location of the EMG electrodes was verified in dissection after the completion of the measurements. EMG recordings were made with WPI DAM-50 amplifiers operating with a low-pass filter of 3 kHz and a high-pass filter of 10 Hz.

Frogs were allowed to recover from surgery for one day, and measurements were taken for 2–3 days following surgery. Jumping measurements were made in an enclosed jumping area approximately 40 cm wide by 2 m long. Lightweight, 1.5 m-long leads were connected to the recording transducers using small multi-pin connectors (Microtech, Boothwyn, PA, USA). The total mass of these leads was less than 2% of the mass of the frog, and care was taken to ensure that leads moved freely and did not interfere with jumping. Sonomicrometer and EMG signals were recorded at 4000 samples per second using a MacAdios 12-bit A/D board (GW Instruments, Somerville, MA, USA) in a Macintosh computer. Sonomicrometer signals were filtered in software (Superscope II; GW Instruments) with a 60 Hz smoothing filter. EMG signals were filtered with a 200 Hz high-pass FIR filter. For sonomicrometer measurements, the length of the muscle prior to the jump was used as the resting length, L_o, of the muscle. Muscle velocity was calculated from the differentiated length signal. Velocity traces were filtered in software using a 130 Hz smoothing filter (Superscope II).

Measurements of center of mass dynamics

Animals were videotaped with an NAC 200 high-speed video camera operating at 500 frames s^{-1}. Animals were videotaped in lateral view, and only those jumps that occurred in the sagittal plane were used for analysis. Video measurements were synchronized to sonomicrometry and EMG measurements by means of a square-wave signal that appeared on the videotape at the onset of computer data acquisition. Video recordings were digitized into computer and analyzed using NIH Image software. The point of entry of the sonomicrometer leads was used as a marker to estimate the movements of the center of mass. This point is a good estimate of the location of the center of mass (Marsh and John-Alder, 1994; Hirsch, 1931). These video measurements do not account for the distal movement of the center of mass as the legs extend during a jump. We feel that this approximation is appropriate for the following reasons. First, the movement of the center of mass is relatively small. Hirsch (1931) estimated that the center of mass remained in the middle two-thirds of the urostyle in *Rana ridibunda*. Second, most of the movement of the center of mass occurs in the first two-thirds of the jump, because the ankle is the last joint to extend and the foot is quite light. Third, kinematic data may actually underestimate peak power late in the jump due to the effects of smoothing. Thus, the important aspects of the frog jump, with force, velocity and power all peaking late in the jump, are accurately reproduced by our data.

Estimates of the position of the center of mass were used to calculate the force acting on the body and the center of mass velocity and power. Position data were smoothed using a smoothing spline interpolation in the software application Igor (Wavemetrics, Lake Oswego, OR, USA). Data were interpolated to a wave of 1000 points (from approximately 100) with a standard deviation of 0.0015 m. This method is similar to the cubic spline algorithm recommended by Walker (1998) for calculating accelerations from position data. Smoothed position data were differentiated to calculate center of mass velocity, and these data were differentiated to calculate force in the horizontal (fore aft) and vertical planes (Marsh and John-Alder, 1994). Power was calculated from the rate of change of the sum of horizontal and vertical kinetic energies and potential energy.

Overview of the model

A computer-aided engineering application, Working Model (Knowledge Revolution, Redwood City, CA, USA), was used to design a model that simulated the key mechanical features of a muscle–tendon-powered acceleration. The model simulated a muscle–tendon unit that operated across a lever system to move a mass (Fig. 1). The muscle actuator had force–velocity, length–tension and activation properties, and the spring was modeled as a simple linear Hookean spring. Between the muscle and the load to be accelerated was a gearbox through which the effective mechanical advantage (EMA) could be adjusted throughout the contraction to simulate a change in the muscle's leverage against the load. To operate the simulation, the muscle was activated and allowed to shorten over 30% strain. The velocity, power and acceleration of the load were determined only by the properties of the muscle actuator; no other controls over force or velocity were included. These features together modeled a jumping frog as a single muscle operating across a single joint to accelerate the body mass. This model does not

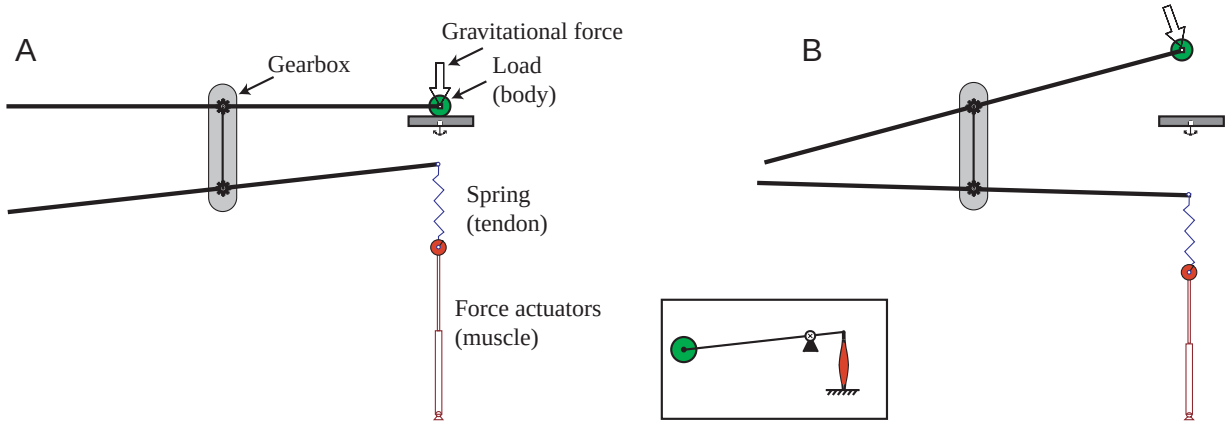

Fig. 1. A diagram of the model for muscle-powered accelerations at rest (A) and during a contraction (B). To simulate a muscle–lever–load system (inset) with an effective mechanical advantage that could vary during the contraction, the muscle–tendon unit operated across a gearing system that included a controllable gearbox to accelerate a load. The muscle consisted of several actuators acting in parallel to produce muscle force–velocity, length–tension and activation properties. The movement was subject to inertial and gravitational forces. The properties and dimensions of the muscle and the load were chosen to approximate the entire hindlimb and body of a jumping frog.

address multi-joint coordination of muscle forces or the effects of limb inertia, or potential variation in muscle activation. The muscle model does address the key features of the dynamic interaction between muscle force–velocity properties, elasticity, muscle mechanical advantage and the dynamics of an accelerating load. A preliminary version of this model was described by Marsh (1999). The model and documentation are available online (http://jeb.biologists.org).

Model muscle and load

The muscle actuator was constructed from several actuators operating in parallel to produce the proper activation timing, force–velocity and length–tension properties during a contraction. Central to the muscle actuator was the force–velocity actuator, which developed force F_{fv} in proportion to its shortening velocity following a simple Hill-type equation:

$$F_{fv} = \frac{P_o(1 - V_m/V_{max})}{V_m/0.37V_{max} + 1} , \quad (1)$$

where V_m is muscle shortening velocity and V_{max} is the maximum muscle shortening velocity (both in m s^{-1}). P_o is the peak tetanic tension (in N). The constant 0.37 defines the curvature of the force–velocity relation; this value gave the best fit to force–velocity data from *Rana catesbeiana* sartorius muscle (R. L. Marsh, unpublished data). For the equations and results presented here, positive values represent actuator shortening.

To achieve muscle activation and length–tension behavior, actuators were stacked in parallel to act in opposition to the force–velocity actuator. We assumed that muscle activation increased linearly over the first 20 ms of muscle contraction. This effect was achieved by an actuator that resisted the force–velocity actuator during the first 20 ms of contraction with force F_{act} that decreased linearly with time (t):

$$F_{act} = -F_{fv}(1 - 50t); \quad t<0.02 . \quad (2)$$

This actuator resisted the force produced by the force–velocity actuator such that, during the first 20 ms of contraction, the force output of the two actuators depended both upon the shortening velocity (equation 1) and upon the level of activation. The actuator was turned on or off according to the conditional $t<0.02$ s. Muscle deactivation was not included in the model. Including muscle deactivation would have made it difficult to achieve identical excursions under different model conditions. Because deactivation is a function of time, the total muscle strain would vary according to the final muscle velocity at the onset of deactivation.

Length–tension properties were modeled by stacking actuators in parallel with the force–velocity actuator. Two actuators (F_{LT1} and F_{LT2}**)** were used to model the length tension effect:

$$F_{LT1} = -F_{fv}(0.97 - 1.09L_m/L_o); \quad 0.74<L_m/L_o<0.89 , \quad (3)$$

$$F_{LT2} = -F_{fv}(3.67 - 4.72L_m/L_o); \quad L_m/L_o<0.74 , \quad (4)$$

where L_m is muscle length and L_o is resting muscle length, in meters. These actuators resisted the force–velocity actuator in proportion to the length of the actuators, to simulate the length–tension relation described by Gordon et al. (1966) for frog semitendinosus. For example, at a length of $0.8L_o$, F_{LT1} would effectively reduce the muscle force output by 10%. We defined the transition from the plateau region to the descending limb of the length tension relation as L_o, and all simulated contractions started at this length. Together, the length, force–velocity and activation actuators operated independently to influence force output of the simulated muscle, F_m, during the contraction:

$$F_m = F_{fv} + F_{act} + F_{LT1} + F_{LT2} . \quad (5)$$

The dimensions and contractile properties of the model muscle were chosen to represent the musculature of the hindlimb of a bullfrog as a single muscle. The maximal

shortening velocity (V_{max}), maximal stress (P_o) and curvature of the force–velocity curve were determined from the force–velocity properties measured in isolated sartorius of *Rana catesbeiana* (Marsh, 1994). A Q_{10} of 2 for maximal shortening velocity was used to calculate a V_{max} of 9 L s^{-1} for the frogs at temperatures measured in the present study (mean temperature = 26°C). It was assumed that the muscle generated 30 N cm^{-2} peak isometric stress. The tendon was modeled as a linear spring. Tendon stiffness was chosen such that a force equivalent to P_o would give a tendon extension equivalent to 20% of muscle fiber length. Measurements of muscle shortening *in situ* using sonomicrometry indicated that plantaris muscle fascicles shortened by 10–20% in tetanus when the muscle–tendon unit was held isometric.

Dimensions of the modeled muscle were chosen to produce a single muscle that represented the average dimensions of the hindlimb musculature. Dimensions from dissection of a 210 g frog were used. A total muscle cross-sectional area of 4 cm^2 was used as the estimate for two frog hindlimbs, based on the approximate average of the cross-sectional areas of the ankle, knee and hip muscles, which were 1.9 cm^2, 2.1 cm^2 and 2.2 cm^2, respectively. The muscle cross-sectional area was used to calculate the peak isometric force from the peak isometric stress value given above. The length of the model muscle was based on the sum of the lengths of the hindlimb muscle fascicles, which averaged 36 mm, 26 mm and 19 mm for the hip, knee and ankle, respectively. The total muscle mass was 36 g for two legs.

The load meant to simulate the body of an accelerating frog was 210 g, the mass of the frog used for muscle dimension measurements. A gravitational force equivalent to 0.5 times gravity acted against the load. This value was chosen because it represents the component of the gravitational force that acts, on average, against the direction of movement for a jump with a trajectory of 30° to the horizontal. In an actual frog jump, the animal may work more or less against gravity depending on variation in instantaneous trajectory during the takeoff phase. Because the load moved along a circular trajectory, gravitational forces were modeled with a constant force vector that rotated along with the lever on which the load was mounted.

Effective mechanical advantage (EMA)

The leverage with which a limb muscle produces force against the ground can be described by its EMA; the ratio of the distance from the muscle line of action to the joint center of rotation, or muscle moment arm *r*, and the orthogonal distance from the joint center of rotation to the ground reaction force vector, or out-moment arm *R* (Biewener, 1989). The effective mechanical advantage (EMA) that muscles operate with, on average, over the course of the jump can be estimated from the ratio of total muscle shortening to the distance the body moves. For the frog used to determine muscle dimensions, the total hindlimb length was approximately 200 mm. It was assumed that muscles involved in jumping contracted over a strain of 30% during a jump. This gives a total muscle shortening of 0.3×80 mm=24 mm, and a mean EMA of 24/200=0.12.

All model simulations were performed at the same mean EMA; i.e. the load always moved the same total distance for the complete contraction. However, to model the effect of a variable EMA throughout the jump, the muscle–lever system operated through a controllable gearbox. This gearbox controlled the ratio of output (body) velocity to input (muscle) velocity, or the reciprocal of EMA, and could therefore simulate changes in EMA that might occur with either a change in *R* or *r*. For fixed EMA contractions, the gearing was held constant throughout the contraction. For variable EMA contractions, an equation was used to vary the gear (1/EMA) as a function of the length of the muscle–tendon unit (L_{mt}) or velocity of the body (V_b). Gearing was controlled by an equation for two variable EMA conditions. First, the gear was controlled as a function of velocity of the load such that the muscle shortening velocity was maintained at $0.3V/V_{max}$:

$$\text{Gearing} = V_b/0.3V_{max} . \quad (6)$$

For this simulation, the gear was maintained at 2 during the early part of the contraction when zero or low values of V_b would have resulted in unreasonable gear values. Equation 6 results in a steadily increasing gearing, or steadily decreasing EMA, during the simulated jump.

The second equation was chosen to allow a continuously decreasing gearing throughout the jump:

$$\text{Gearing} = 1/(0.7 - 5.3L_{mt}) . \quad (7)$$

This equation resulted in a variable EMA that was nearly the opposite of equation 6. That is, the EMA increased in direct proportion to velocity of the body during the contraction. Both equation 6 and equation 7 resulted in a mean EMA of 0.12 for the entire contraction.

Model configurations

We compared the performance of the model in five different configurations. In all of the configurations, the load and muscle contractile properties were the same. The model configurations differed in the presence/absence of a series elastic component and the EMA trajectory:

(1) Stiff, constant; simulated the action of a muscle with no series elastic element operating with constant leverage.

(2) Stiff, increasing; simulated the action of a muscle with no series elastic element operating with increasing leverage (EMA) as the contraction progressed.

(3) Stiff, decreasing; simulated the action of a muscle with no series elastic element operating with decreasing leverage as the contraction progressed; the leverage was adjusted to maintain muscle shortening at 30% of maximum, the velocity of maximum power output.

(4) Compliant, constant; simulated the action of a muscle–tendon unit operating with constant leverage.

(5) Compliant, increasing; simulated the action of a muscle–tendon unit operating with increasing leverage as the contraction progressed.

To simulate the contraction in each configuration, we ‘stimulated’ the muscle to fully activate while the load was at rest. The muscle contracted, producing force according to the combined effects of force–velocity, length–tension and activation properties and the interaction with the inertial and gravitational forces on the load. The simulation was allowed to run until muscle fiber strain reached 30%. Muscle strain, velocity, force and power were recorded during the contraction. We also recorded the velocity and force on the load during the contraction. The total work done on the mass and the kinetic energy work were calculated from the energy values at the end of the simulated contraction.

Results

In vivo *measures of frog jumping*

The dynamics of body movement during the takeoff period for jumping bullfrogs (Fig. 2) were similar to patterns that have been observed in several species of hylid frogs (Marsh and John-Alder, 1994). Velocity of the body increased throughout the jump. The time of peak force occurred from approximately the midpoint of the jump to 70% of the jump period. Peak power outputs also occurred late in the jump. For the two longer (90 cm) jumps shown in Fig. 2, peak instantaneous power outputs are in excess of the power expected from the extensor muscle mass in the hindlimbs. An inclusive measurement of the muscles that might be involved in jumping (Marsh, 1994) gives a hindlimb muscle mass of 17% body mass. If we assume a peak isotonic power output for these muscles of 300 W kg^{-1} muscle, the maximum instantaneous body-mass-specific muscle power output expected for the frogs in this study would be approximately 50 W kg^{-1}. The highest instantaneous power outputs we measured in bullfrog jumping were about 1.5 times this maximum instantaneous muscle power. This high power output suggests that redistribution of power by elastic structures is important in bullfrogs, although the enhancement of 1.5 times maximum instantaneous power output is much lower than the values of seven times maximum instantaneous power output observed for smaller hylid frogs (Peplowski and Marsh, 1997).

Our measurements of muscle shortening revealed a characteristic bimodal pattern of shortening velocity in bullfrog plantaris during jumping (Fig. 3). In jumps greater than 60 cm (Fig. 3A–C), active muscle fascicles shortened rapidly early in the jump and late in the jump, with a region of reduced velocity during mid-jump. This pattern was not observed in some shorter jumps, where muscle velocity showed a slow decline or was approximately constant during takeoff (Fig. 3D–F). In some cases, the two peaks in muscle shortening velocity corresponded to two separate EMG bursts. More commonly, the EMG activity was approximately constant or gradually increased during the takeoff phase (Fig. 3). The total muscle strain for all jumps greater than 60 cm was 26.4±0.3% (mean ± S.E.M.; N=5 animals).

Comparison of muscle shortening with body movement during powerful jumps reveals that much of the shortening of the plantaris occurred before significant movement of the body (Figs 4, 5). Generally, the pattern of muscle shortening did not resemble the pattern of body movement (Fig. 4). Fig. 4A,C shows that muscle fascicle velocity reached a maximum when body velocity had just begun to increase. During much of the period when body velocity increased, muscle fascicle shortening velocity decreased. The increase in muscle shortening velocity late in the takeoff phase is more consistent with the increase in velocity of the body observed during this period. Figs 4B,D, 5 illustrate the lack of correlation between muscle shortening distance and the movement of the body. For the jumps shown, half of the shortening of the muscle

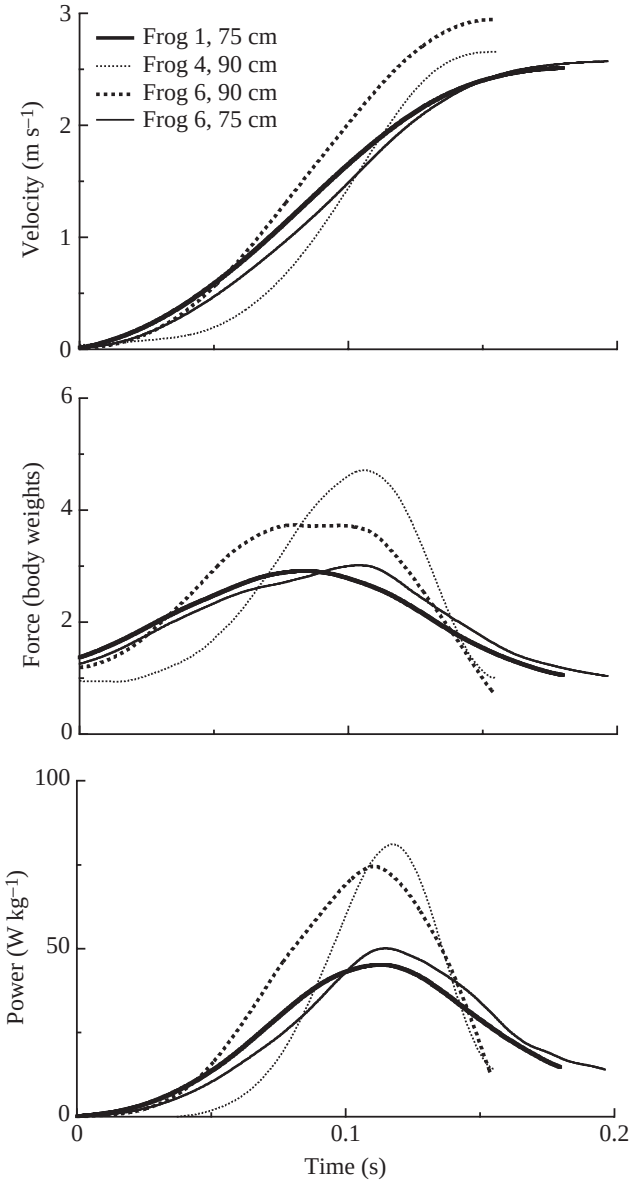

Fig. 2. The velocity, force and power of the center of mass of four frog jumps, as determined from high-speed video analysis. Time zero on the graphs was taken as the time of the beginning of electromyographic activity in the plantaris muscle. Takeoff angles for all four jumps were between 20° and 40° from the horizontal.

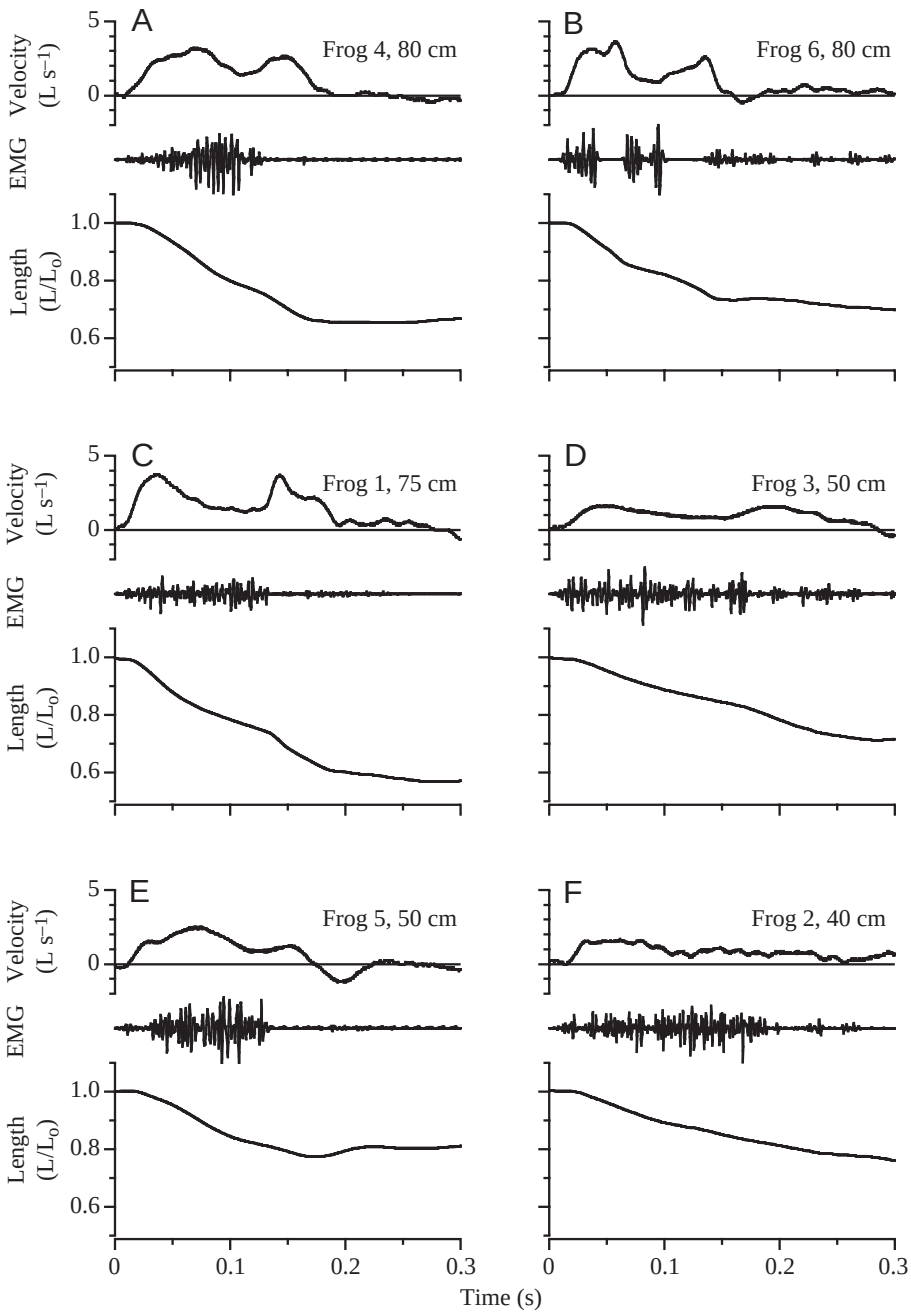

Fig. 3. Fascicle velocities, lengths and electromyographic activity of the plantaris muscle for six jumps of differing lengths: (A,B) 80 cm, (C) 75 cm, (D,E) 50 cm, (F) 40 cm. Longer jumps are characterized by a bimodal pattern of shortening velocity, with the fastest velocities occurring early and late in the jump.

fascicles occurred before significant movement of the body (Figs 4B,D, 5). The lack of correlation between muscle fascicle movement and body movement suggests that muscle shortening early in the jump occurs against stretching elastic elements. Muscle fascicle shortening early in the jump in the plantaris is not due to early extension of the ankle joint (Fig. 5). Kinematics of jumping bullfrogs show that ankle extension begins at the same time or later than extension at other joints (Calow and Alexander, 1973).

Model results

To determine whether the patterns of body movement and muscle shortening in jumping frogs were consistent with the mechanical behavior of muscles and series elastic elements, we modeled jumping as a single contraction of a fully active muscle that contracted by 30% of its length as it accelerated a load (Fig. 1). We compared the velocity, power and force on the modeled load with the same quantities for jumping frogs. These results are shown in Fig. 6 for four of the five model configurations.

The model results show that the patterns of body movement observed in jumping bullfrogs are most consistent with muscle-powered accelerations in which the muscle operates in series with an elastic element and operates through a variable, increasing EMA throughout the acceleration (Fig. 6D). Like the frog jump, this modeled acceleration showed highest forces and powers late in the jump, and peak isotonic powers of approximately 1.5× peak isotonic power. The compliant, increasing EMA configuration also showed a simultaneous increase in both force and velocity during more than half of the jump (Fig. 6D, top two panels) and resulted in the highest final velocity of the load. The agreement between model body movement and frog movement was also good when the model muscle included a series elastic element and a constant EMA (Fig. 6C). When the model muscle operated without a series elastic element (Fig. 6A,B), the timing of force, velocity and power applied to the body was not consistent with the pattern observed during frog jumping. Both non-compliant model configurations produced a force peak early (Fig. 6A,B, middle panel), with force declining throughout most of the contraction. The decline in output force was due to force–velocity effects in the model with constant EMA (Fig. 6A). When the model operated with a continuously decreasing EMA to maintain a constant muscle shortening velocity, the force applied to the body decreased throughout the contraction as a result of the decreasing leverage (Fig. 6B). In both non-compliant configurations, power outputs were near peak isotonic during much of the contraction but they did not exceed it.

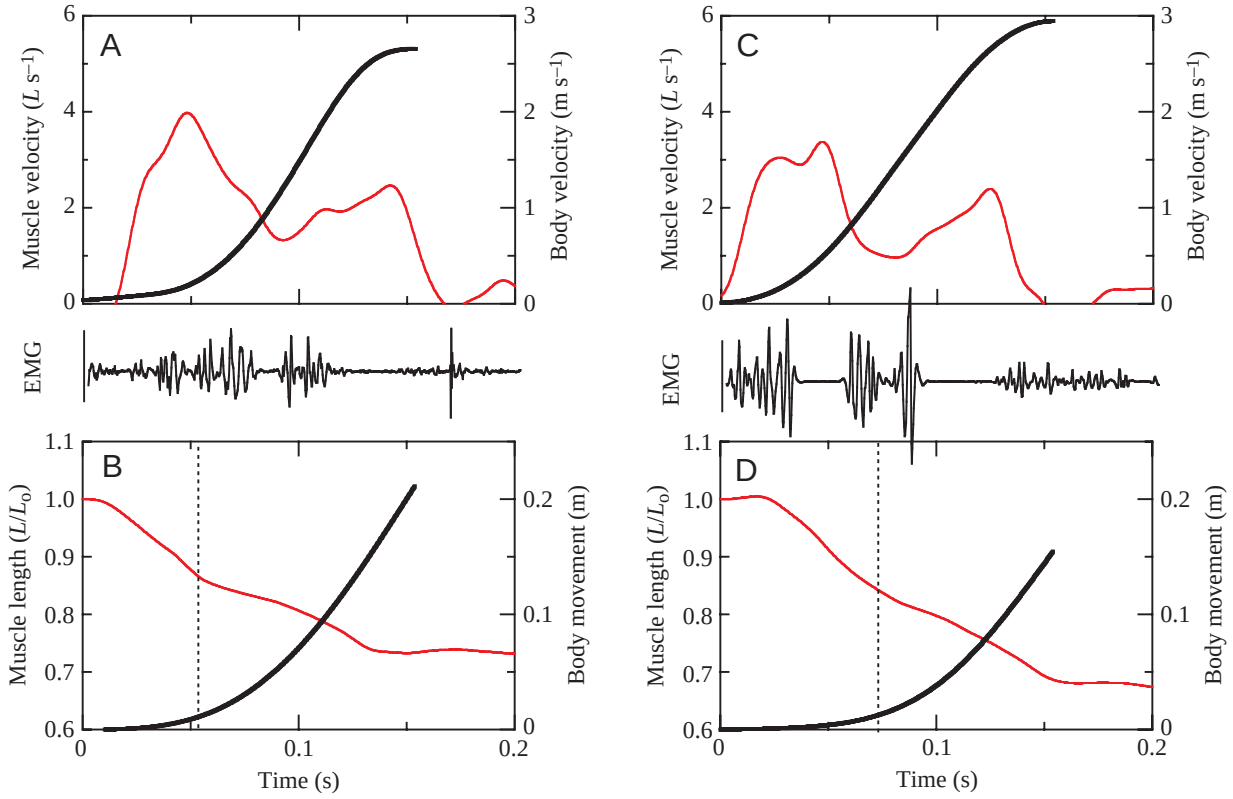

Fig. 4. A comparison of the movement of the body (thick black lines) with the shortening of the plantaris muscle fascicles (thin red lines) in two frog jumps (frog 1 and frog 6). The velocity of shortening in the plantaris is independent of the velocity of the body (A,C). Panels B and D contrast the shortening of the plantaris muscle fascicles with the displacement of the body. At the point where half of the muscle fascicle shortening has occurred (vertical broken line), the body has undergone very little displacement. EMG, electromyographic activity.

In addition to the pattern of movement of the model load, we also compared the pattern of shortening in the model muscle to that observed for the plantaris muscle in jumping frogs. The different model configurations resulted in strikingly different patterns of muscle shortening and force (Fig. 7). Without a series elastic component, muscle velocity increased in parallel with body velocity throughout the contraction (Fig. 7A), and muscle force declined during most of the contraction due to force–velocity effects (Fig. 7A, middle panel). When EMA was adjusted to hold shortening velocity constant, muscle force and power output were nearly constant throughout the contraction, except for the decline due to length–tension effects (Fig. 7B). When a series elastic component was present, muscle shortening velocity was high early in the contraction as the muscle shortened against the stretch of the series elastic component, then declined as force began to reach a maximum and the spring no longer stretched (Fig. 7C,D). During the last part of the contraction, an increase in both tendon and muscle velocity contributed to the increase in velocity of the load. Under these conditions, muscle velocity bore little resemblance to load velocity during much of the acceleration. The bimodal pattern of muscle shortening velocity observed for the models that included a series elastic element was very similar to that observed for the plantaris in jumping bullfrogs (Figs 3, 4). The muscle maintained a relatively high power output during the entire contraction (Fig. 7D, bottom panel), as energy was loaded into the spring during the first half of the contraction and was applied directly to the load during the second half.

The model that most closely reproduced the dynamics of a frog jump also performed the greatest work to increase the velocity of the body. Jump distance is proportional to the velocity of the body at takeoff (as well as takeoff angle), and these results suggest that operating muscles with tendons in series and a decreasing EMA can increase jump distance. Table 1 shows the work performed during jumps for each model configuration. The variable EMA and elastic configuration produced approximately 13% more work than the configuration in which the muscle acts with a constant EMA and no spring.

Discussion

We undertook this study to gain insight into what conditions improve muscle performance when the major task of a muscle is to accelerate a mass. We addressed this issue by combining empirical measurements of frog jumping with modeling. The results demonstrated that the velocity, power and force trajectory observed during frog jumping could be reproduced by a model of a single, fully active muscle–tendon unit

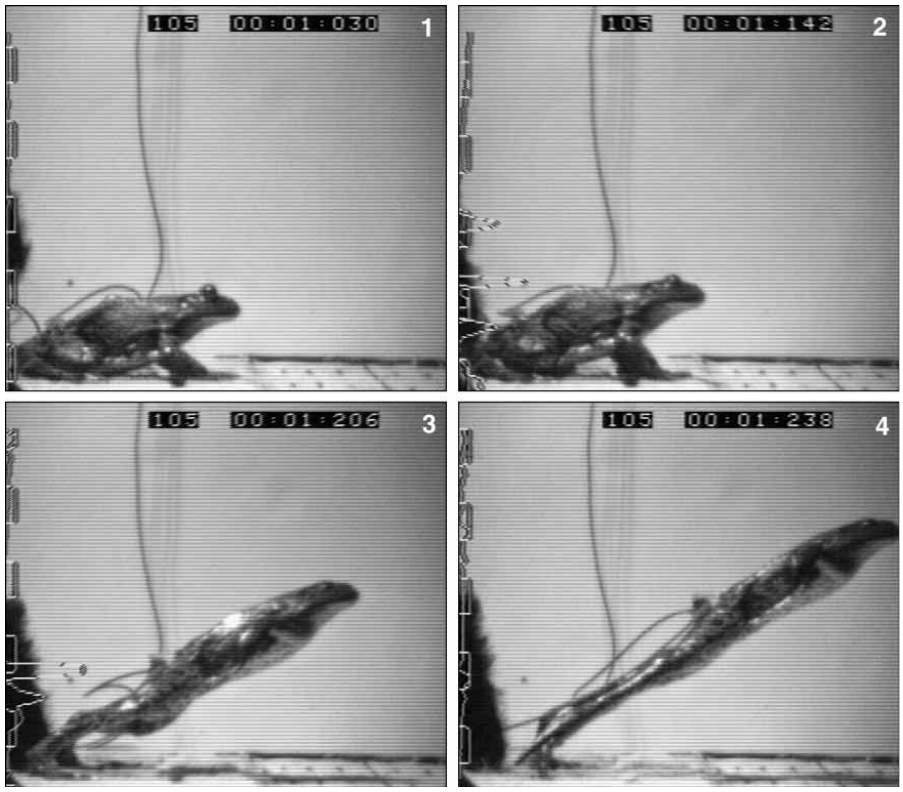

Fig. 5. Four frames from a high-speed video sequence of a frog jump. Frame 2 depicts the point where half of the plantaris muscle fascicle shortening has occurred.

operating against an inertial mass. No external control was required to produce the bullfrog pattern of movement (i.e. recruitment was not varied during the contraction) but the observed pattern of body movement and muscle movement could only be reproduced when the muscle actuator operated in series with a compliant tendon. The pattern of shortening of the muscle and the dynamics of movement of the body were determined not by control of muscle recruitment but by the dynamic interaction of muscle–tendon properties and the inertial and gravitational forces acting on the body. Two consequences of the interdependence of muscle dynamics and body dynamics were observed. First, elastic mechanisms can increase the work that bullfrog muscles do during a jump and therefore increase jump performance. Movements of elastic structures uncouple muscle shortening from body movements and allow muscles to operate at shortening velocities during the contraction that result in greater work output. Second, an increase in EMA throughout the jump may provide an inertial catch mechanism, enhancing storage and release of elastic energy.

A simple acceleration model reproduces the dynamics of a frog jump

When our modeled muscle included a series elastic element, there was a striking agreement between the modeled acceleration and the mechanical behavior of jumping bullfrogs; without a series elastic element many of the features of the jump could not be reproduced. The only inputs to the model were estimates of the dimensions and physiological properties of the muscles involved (peak tetanic force, maximum shortening velocity, etc.), and the remaining behavior of the model resulted from the interaction of these properties with the inertial and gravitational forces on the accelerated load. When the model included a series elastic element and a variable EMA, the model output matched a typical bullfrog jump in jump duration, magnitude and timing of peak force on the body, magnitude and timing of peak power output and pattern of change in body velocity (Fig. 6D). Under these conditions, there was also a remarkable agreement between the pattern of shortening of the modeled muscle and the pattern of shortening measured in the plantaris muscle (Figs 3, 4, 7D). By contrast, without a series elastic element, the model produced peak forces and powers early in the jump, rather than late as observed in frogs, and magnitudes of peak power output were lower than for frogs (Fig. 6A,B). The measured pattern of muscle shortening velocity in the plantaris was not reproduced in models without a series elastic element (Fig. 7A,B).

Table 1. *Model output for five configurations*

Model configuration		Output				
Compliance	EMA	Work (J kg^{-1})	Peak power (W kg^{-1})	Mean power (W kg^{-1})	Peak force (body weights)	Time of peak force (% contraction time)
Stiff	Constant	26.6	280	214	5.2	16
Stiff	Increasing	25.7	280	178	3.4	14
Stiff	Decreasing	27.4	278	233	6.0	8
Compliant	Constant	27.0	356	212	3.8	43
Compliant	Increasing	31.0	429	194	3.2	73

Mass-specific values are presented per unit muscle mass. Peak force and time of peak force refer to the forces applied to the accelerated load.

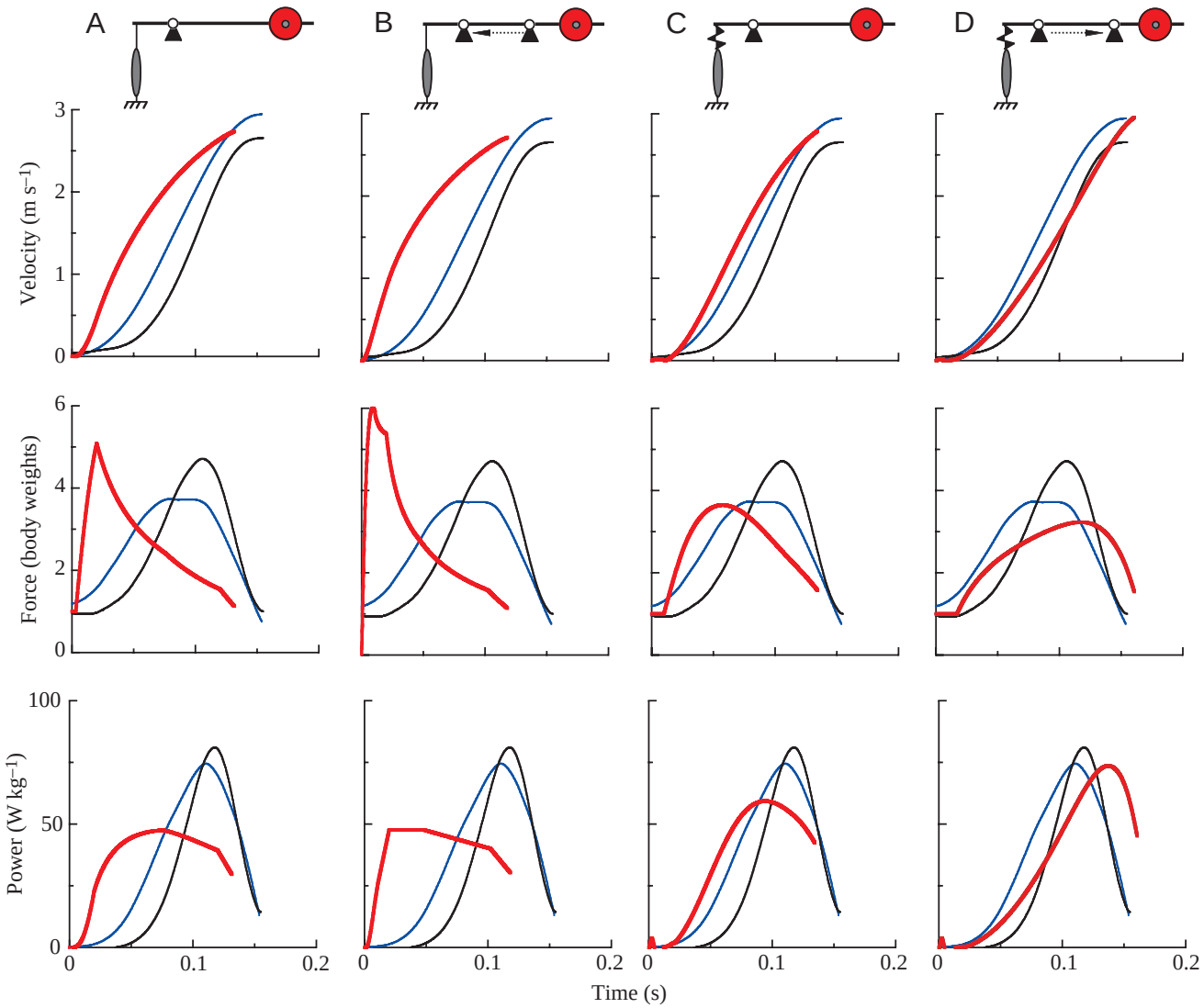

Fig. 6. A comparison of the movement of the modeled load (thick red line) with the movement of the body in the two longer frog jumps shown in Fig. 2 (thin blue and black lines). Each column of graphs presents the velocity, force and power of the load/body for a single contraction under one of four model configurations: (A) no series elastic element, constant effective mechanical advantage (EMA), (B) no series elastic element, decreasing EMA, (C) compliant series elastic element, constant EMA and (D) compliant series elastic element, increasing EMA. The shape of the force, velocity and power curves during jumping in frogs most closely resembles the model configuration shown in D, where the muscle actuator contracts through a series elastic element and a continuously increasing EMA. All model contractions occurred over the same total muscle strain and same total load displacement. Power is expressed in W kg^{-1} body mass.

The results from our model indicate how elastic elements can allow movements that would otherwise be incompatible with the mechanical behavior of fully active muscle contractile elements. In the case of the dynamics of the body in jumping frogs, the simultaneous increase in body force and velocity cannot be powered directly by muscle contractile elements because the force–velocity relation dictates that force must decline as velocity increases. A pattern of decreasing mechanical advantage cannot solve this problem; as EMA decreases to allow a constant muscle velocity, the force applied to the body per unit muscle force must decrease (Fig. 6B). The observation that the appropriate pattern of force and power output could only be reproduced by a model with a series elastic component and a constantly *increasing* EMA illustrates the importance of the interaction of muscle properties and the forces acting on the load.

How should muscles shorten when accelerating inertial loads?

Our model predicts a distinct pattern of muscle fiber shortening during contractions involving an elastic element in series with an inertial load. Initially, shortening velocity is predicted to be high, followed by declining velocity as the spring becomes fully stretched. Later in the movement, shortening velocity increases again as the load is accelerated. During this period of increasing shortening velocity late in

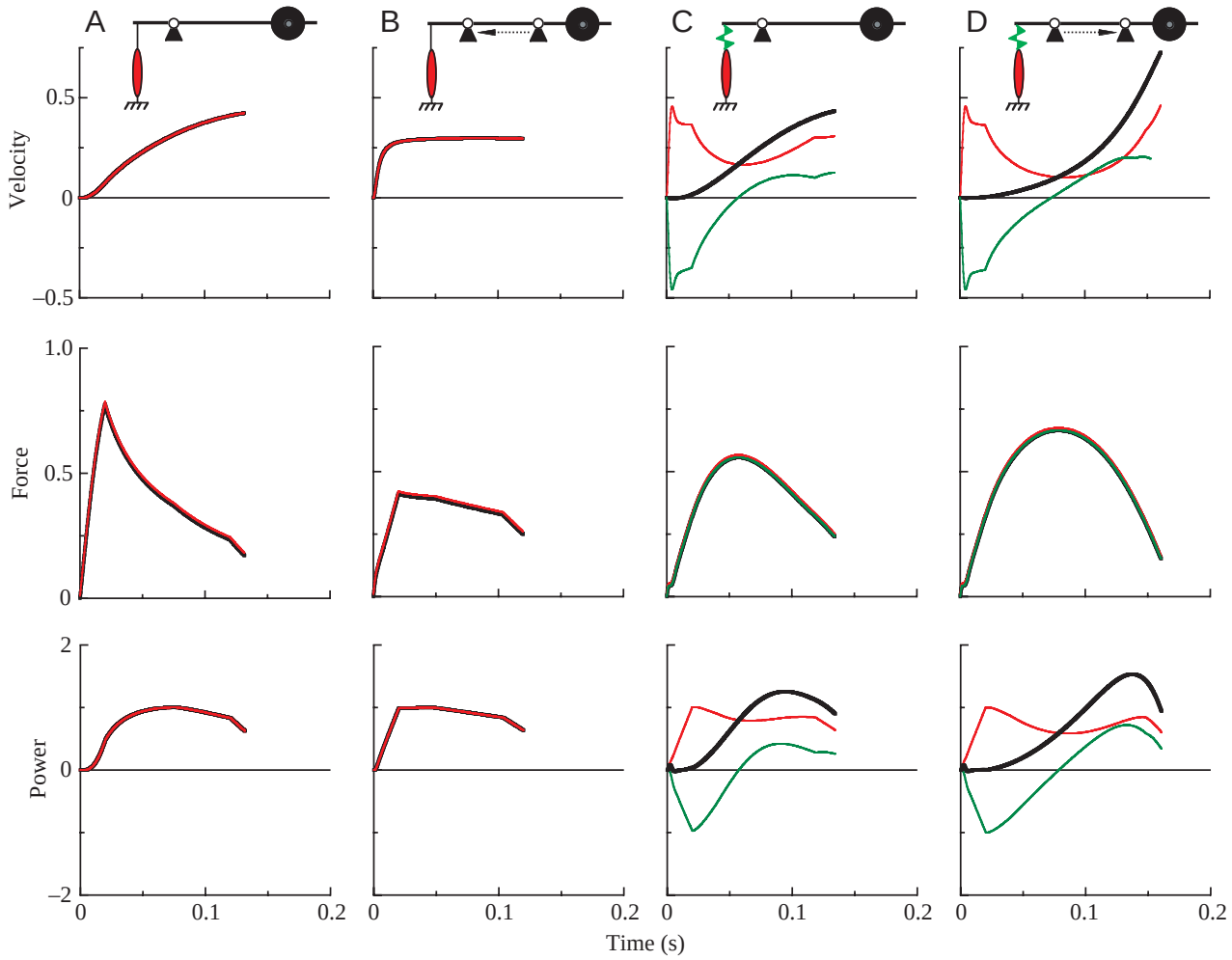

Fig. 7. Velocity, force and power output of the simulated muscle contractile element (thin red line), tendon (green line) and muscle–tendon unit (thick black line) for simulated jumps under the same four configurations as for Fig. 6: (A) no series elastic element, constant effective mechanical advantage (EMA), (B) no series elastic element, decreasing EMA, (C) compliant series elastic element, constant EMA and (D) compliant series elastic element, increasing EMA. All values are expressed relative to the maximum for the modeled muscle. When the muscle operates with a series elastic element (tendon), muscle velocity peaks early in the contraction due to stretch of the elastic element (top panels, C,D). Muscle–tendon power output can exceed peak isotonic power late in the jump due to high power outputs of the recoiling spring (bottom panels, C,D). When EMA is varied to maintain a constant muscle shortening velocity (B), power output is maintained at peak isotonic power until a small decline in force due to length–tension effects.

the jump, muscle forces drop due to force–velocity and length–tension effects and energy is released from the tendon.

The shortening pattern of the muscle fibers in the plantaris, an ankle extensor with a long in-series tendon, agrees with the model predictions. The presence of an elastic tendon uncouples fiber shortening in the plantaris from movement of the body. According to our model, muscle contractile elements perform more work when coupled with an elastic component because they can operate on average at relatively slower velocities and higher forces when shortening. The pattern of muscle shortening velocity measured in the plantaris and predicted by the model to produce high work output is unusual and would have been difficult to predict *a priori* from physiological principles. Not all of the hindlimb muscles in frogs shorten like the plantaris. Previous work has reasonably predicted that jumping animals should operate their muscles at velocities that maximize power, because acceleration requires that force must be produced at the same time that the body undergoes a rapid movement (Hill, 1950b; Lutz and Rome, 1994). Lutz and Rome (1994) found support for this prediction in the shortening pattern of the semimembranosus in leopard frogs (*Rana pipiens*). Their measurements indicated that the leopard frog semimembranosus operated at a constant shortening velocity of approximately 30% V_{max}. Olson and Marsh (1998) also found shortening velocities in the semimembranosus and gluteus medius muscles of bullfrogs that were more uniform than those measured for the plantaris. Thus, proximal muscles with limited capacity for elastic energy storage may not undergo the pattern of shortening observed in the present study. However, results from our model illustrate that a muscle

operating at a constant shortening velocity cannot power movements with the force and velocity trajectory observed in jumping bullfrogs. These results also indicate that the maximum accelerations were not necessarily those with the highest power output (Table 1). We predict that the pattern of shortening observed in the plantaris of jumping bullfrogs is common in frog hindlimb muscles and, more generally, will be found in muscles with substantial in-series tendons specialized to accelerate inertial loads.

Elastic structures improve jumping performance

Our model indicates that bullfrog muscles can power longer jumps by operating in series with elastic elements that store and release the work done by contracting muscle fibers. This is consistent with Alexander's (1995) model demonstrating that compliance in series with a muscle can improve jump height in vertical jumpers over a wide size range. Bobbert et al. (1986) demonstrated that in jumping humans energy loaded into the tendons of the triceps surae early in the jump is released rapidly late in the jump to develop high power output at the ankle. Using a model of the human squat jump, Bobbert (2001) demonstrated that jump performance improved with increasing series elasticity in the triceps surae. Bobbert's results indicated that the series elasticity improved the work output of the hindlimb because it improved the coordination of velocities between segments and maximized the energy applied to the center of mass rather than the limb segments (Bobbert, 2001). Our single-lever model does not address inter-segment coordination but rather indicates that series elastic components can improve muscle work output even in a single muscle accelerating a load. Recently, ultrasound measurements on the gastrocnemius muscle in humans have been used to demonstrate that most of the muscle contractile element shortening occurs against the stretch of elastic elements early in a squat jump (Kurokawa et al., 2001). This observation is generally consistent with the results from the present model, although the gastrocnemius shortening velocity in jumping humans does not show a period of high velocity late in the jump (Kurokawa et al., 2001).

Insect jumpers use a catch mechanism to power jumping in a catapult-like manner, pre-loading elastic energy before any movement and releasing it explosively to power jumping (Bennet-Clark, 1975; Alexander, 1995). Our results suggest that frogs also use a catapult-like mechanism, pre-loading elastic energy in the early part of the jump. Yet there are differences between the catapult mechanism proposed for jumping frogs and that of insects. Bullfrogs appear to perform significant muscle work during the entire jump, whereas in insect jumpers it is thought that the majority of muscle work is performed before body movement during the pre-loading stage (Alexander, 1995; Bennet-Clark, 1975). Our model results also suggest that jumping frogs can pre-load elastic energy in tendons even without a functioning physical catch, although we cannot rule out the possibility that a physical catch mechanism might further enhance elastic energy storage. Simply redistributing the muscle work during shortening by elastic storage (Marsh and John-Alder, 1994) can improve performance.

A variable mechanical advantage provides an inertial catch mechanism

The pattern of continuously increasing EMA during a jump that was most effective for increasing muscle work output in our model may provide an inertial catch mechanism for elastic energy storage and recovery. The physical catch mechanisms employed by insect jumpers provide resistance to allow muscles to contract to a high force without causing movement at a joint (Gronenberg, 1996). The delay in applying force to the body is necessary to stretch the spring. In our model, the inertia of the body early in the jump allows muscle force to rise to a high level before significant displacement of the body occurs. During the period of increasing force, the series elastic element is stretched, and energy is stored. A poor EMA early in the jump enhances this effect, because the force transferred to the body is relatively low and thus accelerations are low. In order to release the energy stored in the elastic elements before the movement is completed, force must necessarily decline. The more rapidly force declines the more rapidly the energy will be released. The increasing EMA as the movement progresses accentuates the rapid increase in muscle fiber shortening, and consequent decline in force, thus facilitating the release of the stored energy.

Importantly, the most effective pattern of change in mechanical advantage in our model is the opposite of the strategy widely accepted as favorable for accelerations. Other workers have suggested that muscular systems ought to be arranged to allow for constant shortening velocity during movement (Lutz and Rome, 1994, 1996; Carrier et al., 1994). To achieve this end, the EMA must decrease during an accelerative movement; i.e. the muscle gearing must continuously increase (Carrier et al., 1994). Many motor-driven machines and human-powered vehicles (e.g. bicycles) utilize this strategy to increase output velocity for a given motor velocity. Our results suggest that for some activities the unique behavior of a muscle motor in series with an elastic element may operate best with a counterintuitive use of variable mechanical advantage, one that decreases the output (body) velocity for a given input (muscle) velocity.

A variable mechanical advantage during muscle contraction has also been proposed as a mechanism to maximize muscle efficiency and power during steady-speed running. Carrier et al. (1998) examined the pattern of mechanical advantage change at individual joints in running dogs and found that the pattern of EMA at the shoulder and knee was consistent with the idea that EMA decreases to maintain a constant muscle velocity. However, they found that at the hip, wrist, elbow and ankle joints the EMA increased during the contraction. Thus, the pattern of EMA at some joints in running dogs resembles the pattern predicted by our model to maximize work output in a muscle–tendon unit acting to accelerate an inertial load. However, during running, muscles do not operate at maximal power or work outputs (Farley, 1997), and the accelerations of

the body powered by a single muscle contraction are relatively small. It has been suggested that the design of the musculoskeletal system may favor minimization of muscle work during running to improve energy economy (Taylor, 1994; Roberts et al., 1997). Therefore, although the pattern of EMA change at some of the joints in running dogs may resemble that suggested for jumping frogs, it remains to be seen whether the pattern of decreasing EMA that maximizes work output in our model of contraction will apply generally to activities where maximum work is not the desired mechanical output.

Model constraints

In modeling, a trade-off often exists between complexity and generality. Our goal was to capture in a simple form the essential features of an accelerative contraction driven by skeletal muscle. This simple model accurately characterizes the complex interaction of the properties of a single muscle, tendon and lever with the inertial and gravitational forces acting on an accelerated mass. The model does not include the coordinated function of many muscles operating over several joints. Undoubtedly, some of the dynamics of any particular type of acceleration, such as a frog jump, result from the variation in muscle properties, architecture and gearing for individual muscles at different joints. Anatomically precise models of frog jumping are providing, and will continue to provide, insight into the importance of the integrated function of multiple muscles for the dynamics of frog jumping (Kargo et al., 2002; Kargo and Rome, 2002).

Because our goal was to determine maximal muscle performance under conditions of constant muscle strain, our model did not include a muscle deactivation function. Deactivation is time dependent, and other model parameters influenced the time to complete the contraction. Thus, including deactivation would have resulted in variation in total muscle strain between conditions (depending on the velocity of the muscle at the onset of deactivation). Deactivation would have improved the performance of the compliant configurations because it would have allowed the release of all of the stored elastic energy. The model also did not include any regulation of level of muscle recruitment during a jump; it was assumed that the entire muscle mass was fully stimulated at time zero and, after an initial period of activation, was maintained at full activity throughout the jump. The very high power and work outputs observed during some jumps suggest that full muscle recruitment is a reasonable assumption. However, clearly, the level of activation in frog muscles can be modulated to produce jumps of differing distances. During some frog jumps measured, distinct bursts of EMG activity occurred, suggesting that activity may be modulated to fine-tune the jumping movement. Because we were interested in the limit to performance set by muscle contractile properties, we did not attempt to model any modulation in activity during the jump. The functions used to set EMA during our modeled contraction were chosen to represent two extremes. The first function modeled the pattern of EMA that has been proposed for accelerative contractions, where EMA decreases in proportion to the velocity of the body to maintain constant muscle velocity. To facilitate comparison, the other EMA function was effectively the reciprocal of this function, i.e. mechanical advantage increased in direct proportion to the velocity of the load. Experimentation with other functions for the increase in EMA did not result in dramatically different performance of muscle work. In a jumping animal such as the bullfrog, the exact pattern of EMA at any given joint will depend upon how the muscle moment arm changes with joint angle and how the ground reaction force moment arm changes throughout the jump. Although the exact function is unknown, all joints probably experience a decreasing ground reaction force moment arm throughout the jump as leg straightening causes the legs to move towards the midline, shortening the out-lever arm (the distance between the ground reaction force and the joint center of rotation). Thus, a pattern of increasing EMA is not only advantageous for work production during jumping but may also be a necessary consequence of powering jumping with jointed limbs that must transition from fully flexed to nearly straight during a jump.

All simulated accelerations were performed at a single value for mean EMA realistic for a jumping frog. Model simulations at mean EMAs other than the one used here indicate that the magnitude of performance benefit from an elastic mechanism is sensitive to the value of mean EMA used. At higher effective mechanical advantages, the increase in muscle work output when an elastic component is included was greater than the 15% enhancement observed in the present results. At lower EMAs, the increase in work between these conditions was lower. However, at EMAs lower than those used for the simulations presented here the force produced against the body was less than two times body weight throughout the contraction. Such low forces would be inconsistent with powering rapid jumps (Marsh, 1994).

Patterns of work and power output in jumping frogs

The observation that frogs jump farther than they should is based upon the discrepancy between the measured capacity for power production in their hindlimb musculature and the power produced during the takeoff phase of a jump (Marsh and John-Alder, 1994; Peplowski and Marsh, 1997; Navas et al., 1999). A similar discrepancy in power output has been measured in a small mammalian jumper, the galago (*Galago senegalensis*; Aerts, 1997). The present results support the proposal (Marsh and John-Alder, 1994) that this discrepancy can be explained in jumping bullfrogs by the release of elastic energy late in the jump. Peak power outputs during maximal jumps in bullfrogs were approximately 1.5 times their estimated peak muscle power, and the peak power output of the muscle–tendon unit in our model was also 1.5 times the peak muscle power (Table 1). The largest documented discrepancy in power output in jumping frogs was recorded in Cuban tree frogs (Peplowski and Marsh, 1997). Calculations of takeoff power suggest that Cuban tree frogs develop average powers in excess of seven times their capacity for muscle power production. The

power amplification for bullfrogs was much less than this value. However, results from the same model with muscle and body parameters scaled to values appropriate for Cuban tree frogs indicate that a sevenfold power amplification can be obtained with an elastic element and the inertial catch mechanism proposed here (T. J. Roberts and R. L. Marsh, unpublished).

Conclusions

Much of the design of the non-muscular components of the musculoskeletal system has likely been shaped through evolution by the limits to performance imposed by the rather conservative contractile properties of skeletal muscle. Thus, muscles, their naturally occurring loads and the linkages between these two must be approached as integrated systems.

In the present study, this integrated approach yielded the following conclusions about muscle-powered accelerations:

(1) placing an elastic element in series with the muscle enhances performance not only by increasing peak power output but also by increasing work output;

(2) elastic mechanisms may allow muscles to power accelerative movements with force and velocity trajectories that are inconsistent with the mechanical behavior of muscle contractile elements;

(3) arranging the system so that the EMA of the muscle is poor at the beginning of contraction and increases throughout the movement improves performance by enhancing elastic storage and release of energy, i.e. acting as an inertial catch; and

(4) because of the conservative characteristics of skeletal muscle, we predict that elastic mechanisms may play an important role in enhancing muscle power output for maximal accelerations.

We thank Eunice Chung for help with data collection. Peter Weyand provided valuable comments on an early version of the paper. Supported by NIH grants AR39218 and AR47337 to R.L.M. and AR08380 and AR46499 to T.J.R.

References

Aerts, P. (1997). Vertical jumping in *Galago senegalensis*: the quest for an obligate mechanical power amplifier. *Phil. Trans. R. Soc. Lond. B* **353**, 1607-1620.

Alexander, R. McN. (1988). *Elastic Mechanisms in Animal Movement*. Cambridge: Cambridge University Press.

Alexander, R. McN. (1995). Leg design and jumping technique for humans, other vertebrates and insects. *Phil. Trans. R. Soc. Lond. B* **28**, 235-248.

Bennet-Clark, H. C. (1975). The energetics of the jump of the locust *Schistocerca gregaria*. *J. Exp. Biol.* **63**, 53-83.

Bennet-Clark, H. C. (1977). Scale effects in jumping animals. In *Scale Effects in Animal Locomotion* (ed. T. Pedley), pp. 185-201. New York: Academic Press.

Bennet-Clark, H. C. and Lucey, E. C. (1967). The jump of the flea: a study of the energetics and a model of the mechanism. *J. Exp. Biol.* **47**, 59-67.

Biewener, A. A. (1989). Scaling body support in mammals: limb posture and muscle mechanics. *Science* **245**, 45-48.

Bobbert, M. F. (2001). Dependence of human squat jump performance on the series elastic compliance of the triceps surae: a simulation study. *J. Exp. Biol.* **204**, 533-542.

Bobbert, M. F., Huijing, P. A. and van Ingen Schenau, G. J. (1986). An estimation of power output and work done by the human triceps surae muscle–tendon complex in jumping. *J. Biomech.* **19**, 899-906.

Calow, L. J. and Alexander, R. McN. (1973). A mechanical analysis of a hind leg of a frog. *J. Zool. Lond.* **171**, 293-321.

Carrier, D. R., Gregersen, C. S. and Silverton, N. A. (1998). Dynamic gearing in running dogs. *J. Exp. Biol.* **201**, 3185-3195.

Carrier, D. R., Heglund, N. C. and Earls, K. D. (1994). Variable gearing during locomotion in the human musculoskeletal system. *Science* **265**, 651-653.

Evans, M. E. G. (1972). The jump of the click beetle (Coleoptera, Elateridae) – a preliminary study. *J. Zool. Lond.* **167**, 319-336.

Farley, C. T. (1997). Maximum speed and mechanical power output in lizards. *J. Exp. Biol.* **200**, 2189-2195.

Gordon, A. M., Huxley, A. F. and Julian, F. J. (1966). The variation in isometric tension with sarcomere length in highly stretched vertebrate muscle fibers. *J. Physiol.* **184**, 170-192.

Gronenberg, W. (1996). Fast actions in small animals: springs and click mechanisms. *J. Comp. Physiol. A* **178**, 727-734.

Hill, A. V. (1950a). The series elastic component of muscle. *Proc. R. Soc. London Ser. B* **137**, 273-280.

Hill, A. V. (1950b). The dimensions of animals and their muscular dynamics. *Sci. Prog.* **38**, 209-230.

Hirsch, W. (1931). Zur physiologischen Mechanik der Froschsprunges. *Z. Vergl. Physiol.* **15**, 1-49.

Kargo, W. J., Nelson, F. and Rome, L. C. (2002). Jumping in frogs: assessing the design of the skeletal system by anatomically realistic modeling and forward dynamic simulation. *J. Exp. Biol.* **205**, 1683-1702.

Kargo, W. J. and Rome, L. C. (2002). Functional morphology of proximal hindlimb muscles in the frog *Rana pipiens*. *J. Exp. Biol.* **205**, 1987-2004.

Kurokawa, S., Fukunaga, T. and Fukashiro, S. (2001). Behavior of fascicles and tendinous structures of human gastrocnemius during vertical jumping. *J. Appl. Physiol.* **90**, 1349-1358.

Loeb, G. E. and Gans, C. (1986). *Electromyography for Experimentalists*. Chicago: University of Chicago Press.

Lutz, G. L. and Rome, L. C. (1994). Built for jumping: the design of the frog muscular system. *Science* **263**, 370-372.

Lutz, G. J. and Rome, L. C. (1996). Muscle function during jumping in frogs. I. Sarcomere length change, EMG pattern, and jumping performance. *Am. J. Physiol.* **271**, C563-570.

Marsh, R. L. (1994). Jumping ability of anuran amphibians. In *Advances in Veterinary Science and Comparative Medicine*, vol. 38B (ed. J. H. Jones), pp. 51-111. New York: Academic Press.

Marsh, R. L. (1999). How muscles deal with real-world loads: the influence of length trajectory on muscle performance. *J. Exp. Biol.* **202**, 3377-3385.

Marsh, R. L. and John-Alder, J. B. (1994). Jumping performance of hylid frogs measured with high-speed cine film. *J. Exp. Biol.* **188**, 131-141.

Navas, C. A., James, R. S., Wakeling, J. M., Kemp, K. M. and Johnston, I. A. (1999). An integrative study of the temperature dependence of whole animal and muscle performance during jumping and swimming in the frog *Rana temporaria*. *J. Comp. Physiol. B* **169**, 588-596.

Olson, J. M. and Marsh, R. L. (1998). Activation pattern and length changes in hindlimb muscles of the bullfrog *Rana catesbeiana* during jumping. *J. Exp. Biol.* **201**, 2763-2777.

Peplowski, M. M. and Marsh, R. L. (1997). Work and power output in the hindlimb muscles of Cuban tree frogs *Osteopilus septentrionalis* during jumping. *J. Exp. Biol.* **200**, 2861-2870.

Roberts, T. J., Marsh, R. L., Weyand, P. G. and Taylor, C. R. (1997). Muscular force in running turkeys: the economy of minimizing work. *Science* **275**, 1113-1115.

Taylor, C. R. (1994). Relating mechanics and energetics during exercise. In *Advances in Veterinary Science and Comparative Medicine*, vol. 38A (ed. J. H. Jones), pp. 181-215. San Diego: Academic Press.

Walker, J. A. (1998). Estimating velocities and accelerations of animal locomotion: a simulation experiment comparing numerical differentiation algorithms. *J. Exp. Biol.* **201**, 981-995.

Wilson, R. S., Franklin, C. E. and James, R. S. (2000). Allometric scaling relationships of jumping performance in the striped marsh frog *Limnodynastes peronii*. *J. Exp. Biol.* **203**, 1937-1946.